

# Organic Mixed Ion-Electron Conductivity in Polymer Hybrid Systems

Soumyajit Hazra, Arindam Banerjee,\* and Arun K. Nandi\*

Cite This: *ACS Omega* 2022, 7, 32849–32862

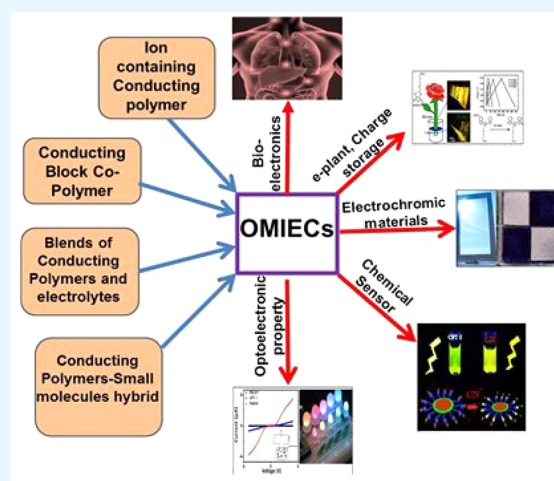
Read Online

ACCESS |

Metrics &amp; More

Article Recommendations

**ABSTRACT:** Recently, organic materials with mixed ion/electron conductivity (OMIEC) have gained significant interest among research communities all over the world. The unique ability to conduct ions and electrons in the same organic material adds to their use in next generation electrochemical, biotechnological, energy generation, energy storage, electrochromic, and sensor devices. Semiconducting conjugated polymers are well-known OMIECs due to their feasibility for both ion and electron transport in the bulk region. In this mini-review, we have shed light on conjugated polymers with ionic pendent groups, block copolymers of electronically and ionic conducting polymers, polymer electrolytes, blends of conjugated polymers with polyelectrolyte/polymer electrolytes; blends of conducting polymer with small organic molecules including conducting polymer–peptide conjugates; and blends of nonconjugated polymers as mixed conducting systems. These systems not only include the well-studied OMIEC systems, but also include some new systems where the OMIEC property has been predicted from the typical current–voltage ( $I$ – $V$ ) plots. The conduction mechanism of ions and electrons, ion–electron coupling, directionality, and dimensionality of these OMIEC materials are discussed in brief. The different properties of OMIEC materials and their applications in diverse fields like energy, electrochromic, biotechnology, sensing, and so forth are enlightened together with the perspective for future improvement of OMIEC materials.



## INTRODUCTION

Materials with efficient coupling between the transport of ionic and electronic charges produce important materials for fabricating a host of technological devices for next-generation optoelectronic, bioelectronic, and energy storage devices.<sup>1a</sup> Organic mixed ionic–electronic conductors (OMIECs) are usually soft polymeric semiconductors that readily solvate ions facilitating ionic species transport along with their electronic conduction. OMIECs are usually water-soluble  $\pi$ -conjugated polymers having the ability to conduct electrons through the conjugated chains together with the flow of ions through a hopping process.<sup>1a,b</sup> The positively charged cations and negatively charged anions are analogous to holes and electrons. However, ionic transport can be more complex; ions can be multivalent, and can form ion pairs and larger clusters; and their flow is very much sensitive to solvation. OMIECs appear in several distinct architectures and the most common type has a blended structure, where a  $\pi$ -conjugated polymer is mixed with a polymer possessing ionic conductivity.<sup>2a,3a</sup> Other architectures include block copolymers,<sup>4a–c</sup> and some homopolymers of conjugated chain with ionic pendent groups and so forth.<sup>5,6</sup> The highly complex phase-behavior of these OMIEC materials deters the fabrication of new synthetic methods leading to poor understanding of the correlation

between the morphology and OMIEC performance. To enable a rational design for improving the OMIEC performance, the interrelation between electronic and ionic conduction (and its adopted suitable morphology) must be well understood, the rigorous study of which is still in its infancy. Some preliminary studies in this regard have started,<sup>2a,3b</sup> but there is still a lack of detailed study to understand the fundamentals of coupling between electronic and ionic conduction in these materials. Thus, new opportunities include the synthesis and design of new macromolecules. Simulation efforts<sup>6</sup> can provide molecular-level insights into the mixed ion electron conductors and their conduction mechanism. Advanced characterization for the real-time monitoring of polymer morphology is also very much essential to delineate the coupled ion-charge transport process.

The current–voltage ( $I$ – $V$ ) characteristics of galvanic cells utilizing mixed ionic electronic conducting polymers are

Received: July 18, 2022

Accepted: August 24, 2022

Published: September 8, 2022



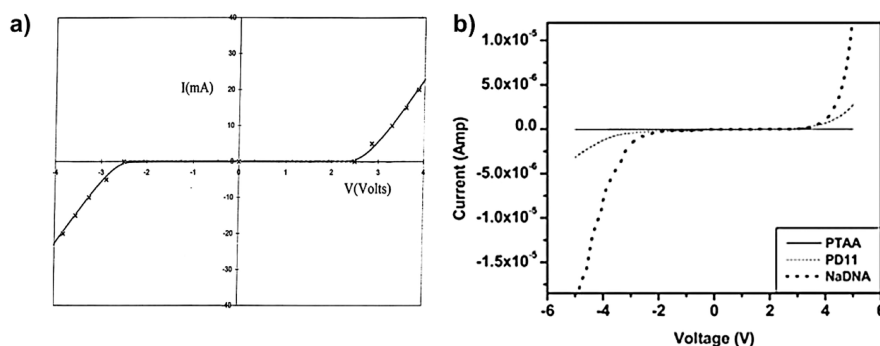
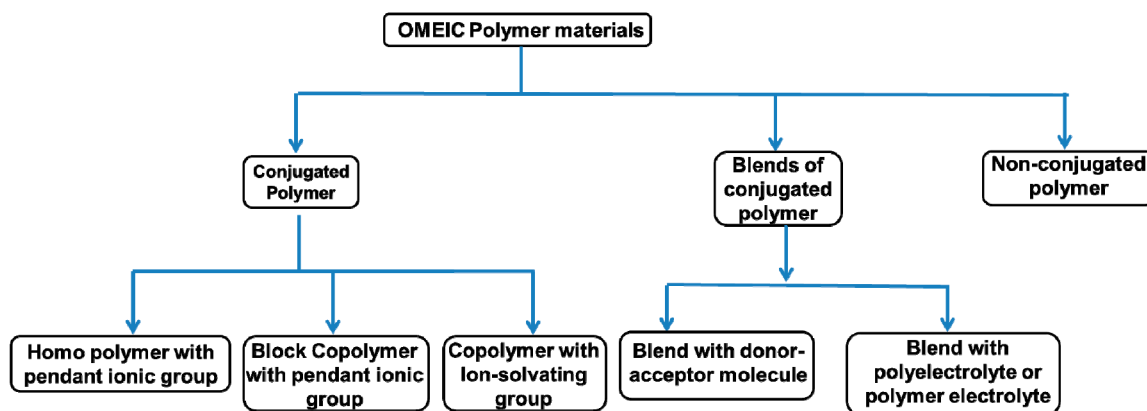


**Figure 1.** a) The characteristic current–voltage ( $I$ – $V$ ) curve of mixed ionic electronic conducting polymers. [Reprinted with permission from ref 7a.] b) Current–voltage ( $I$ – $V$ ) characteristic curves of PTAA, Na-DNA, and PD11 hybrid. [Reprinted with permission from ref 5.]

### Scheme 1. Different Types of Polymeric OMEIC Materials



interesting and are quite different from other semiconductor-<sup>2a,5,7a-c,8</sup> The  $I$ – $V$  characteristic curves arise from diffusion of electrons, ions, molecules, atoms, and charge transfers to/from ions from atoms/ions or vice versa. Specifically, the charge transfer of ions across the electrode/electrolyte interface is of utmost importance along with electronic conduction. Which step is the rate determining one depends on the materials involved, their morphology, and the current density used. Theoretical as well as experimental curves usually show very low current at lower voltages due to flow of only electrons/polarons along the conjugated polymers but at higher voltage the ions begin to move, giving a higher current shown in the shape of a spike<sup>7a</sup> (Figure 1a). Thus, at lower voltage electronic conduction occurs, whereas at higher voltage ionic conduction along with electronic conduction takes place. The mass and size of an ion is a thousand times larger than that of an electron making the mobility of ions slower. So, more energy is necessary for their movement, hence the ionic contribution of current usually occurs at higher voltages through these OMEIC materials. Certain polymer electrochemical cells based on OMEIC blends emit light.<sup>7b-d</sup> The current and light output increase rapidly with voltage. The intensity of light emission increases monotonically with cell current. This can be understood if electrons are indeed injected from one electrode and holes from the other electrode, and a fraction of the electron–hole pairs recombine within the polymer OMEIC emitting light.

A good example of the OMEIC property is noticed in the sodium salt of DNA (Na-DNA), where the electronic conductivity is low arising from electronic flow along the

base pair but in the  $I$ – $V$  curves, at a particular voltage, a sharp hike of current occurs due to conduction by the  $\text{Na}^+$  ions showing OMEIC characteristics<sup>5,8</sup> (Figure 1b). In its blends with poly(3-thiophene acetic acid) (PTAA) at 1:1 composition (PD11), apart from the intrinsic conductivity of PTAA chains there, some additional charge flow may occur between PTAA chains and base pairs of DNA through  $\pi$ – $\pi$  delocalization. Further, transport of  $\text{Na}^+$  ions of Na-DNA may occur through PTAA chains by exchange with the  $\text{H}^+$  of PTAA. Thus, in the  $I$ – $V$  curve of PD11 hybrid there is a moderate signature of OMEIC property but it is absent in pure PTAA.

Generally, OMEIC materials are made with a conjugated backbone for electronic conduction and side chains to aid the ionic intercalation from the operational electrolyte, to assist in the solvation of the processing solvents. In mixed conductor devices, a typical conducting polymer generally used is poly(3,4-ethylenedioxythiophene) doped with poly(styrenesulfonate); (PEDOT:PSS). It has a very high hole conductivity ( $41\,000\text{ S cm}^{-1}$ ), high stability, and is commercially available as a dispersion for solution processing.<sup>9</sup> It is now established that at the bulk, ionic and electronic mobilities are simultaneously affected by processing-induced changes in the nano- and mesoscale structure of PEDOT:PSS films, and an optimal morphology permits the balanced ionic and electronic transport required for mixed conductor devices.<sup>9</sup> Besides, there are some polymer blends and block copolymers that act as OMEIC materials,<sup>1a,2a,3b</sup> showing connectivity between polymer structure, morphology, and ion-electron mixed conductivity. Donor–acceptor polymeric systems play an important role in the OMEIC property of

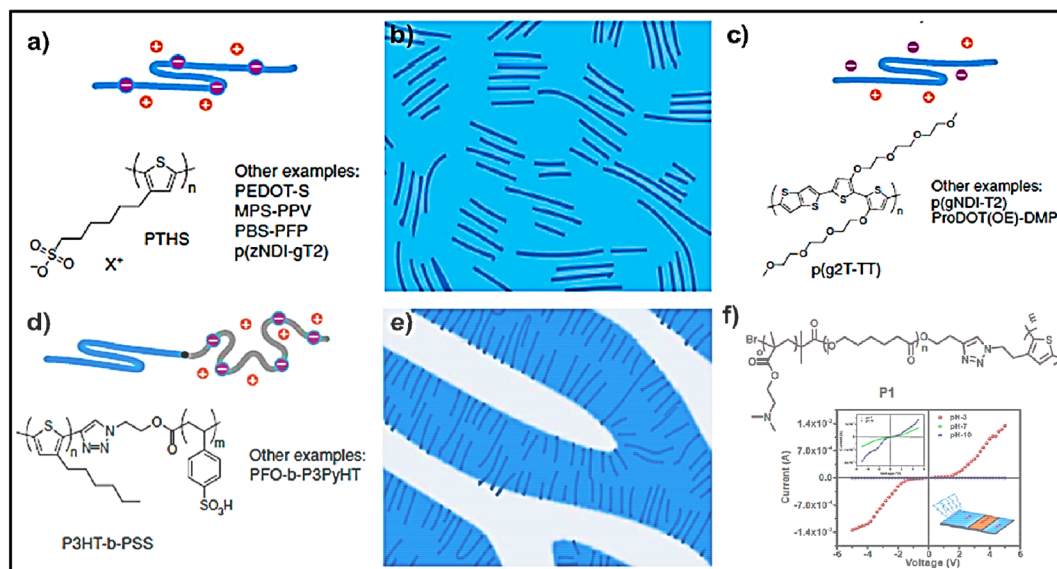


**Figure 2.** (a) Type-1: homo polymer with a charge-conducting backbone and ion-conducting side chain (PTHS), having (b) a uniformly distributed homogeneous conducting state containing both types of conductors (ion and electron), (c) homo polymer with a charge-conducting backbone and ion solvating polymer electrolytes [p(g2T-TT)]; (d) type-2: block copolymer with an electronically conducting conjugated polymer and an ionic charge bearing polyelectrolyte (P3HT-b-PSS), having (e) a phase segregated heterogeneous conducting state containing both types of conductors (ion and electron), (f) pH dependent current–voltage ( $I$ – $V$ ) properties of a water-soluble polythiophene graft block copolymer polythiophene-graft-poly (caprolactone-block-dimethylaminoethyl methacrylate) (PTh-g-PCL-b-PDMAEMA, P1). [Parts a–e reprinted with permission from ref 1a; part f reprinted with permission from ref 19.]

the blends.<sup>2a,b</sup> In polymer-based OMIECs, there is a distinction between polyelectrolytes and polymer electrolytes. The former possesses an ionic moiety that is accompanied by a counter balancing ion. In the latter OMIECs, they are not intrinsically charged, but rather contain polar moieties capable of solvating ions when ionic species are incorporated physically. On the basis of literature reports on polymeric OMIEC materials we classify the OMIEC polymer materials into three main categories which are further classified in subgroups as follows (Scheme 1):

So polymeric OMIEC materials mainly consist of (a) conjugated polymers which may be a homopolymer with a pendant ionic group, block copolymer with a pendant ionic group, copolymer with an ion-solvating group, (b) blends of conjugated polymer with polyelectrolyte/polymer electrolyte, and blends of conjugated polymer having a donor–acceptor interaction. Recently a new class of OMIEC materials has emerged where  $\pi$ -conjugated chains are absent and instead a radical polymer chain is present. In the following section we shall discuss them with a few examples.

Different polymeric OMIEC materials:

(a) Conjugated polymers:

(i) **Homopolymer:** Pure polymers exhibiting mixed ion–electron conduction are achieved by combining known charge-conducting and ion-conducting components into a single polymeric material. Different polymer moieties may be introduced in various ways; **type-1:** homopolymers with an electron-conducting backbone and ion-conducting side chains and **type-2:** as A-B diblock copolymers, where one of the two blocks is ion-conducting, while the other is electron-conducting block. The bulk materials or thin films of type-1 class have relatively uniform distributions of the two types of conductors and both ion and electron

conduction can take place smoothly. In this category, poly[6-(thiophene-3-yl) hexane-1-sulfonate] tetrabutylammonium (PTHS) acts as a mixed conductor where charge transport occurs through a conjugated polythiophene chain and a tetra butyl ammonium ion of sulfonate group is responsible for ionic conduction (Figure 2a). The counter cation may be of different sizes and its ionic conduction depends on the mobility of these ions, and there is no microphase separation between  $\pi$ -conjugated and ion conducting components (Figure 2b). The side chains play a unique role in these OMIEC materials, as they serve as ion shuttles into the film where simultaneous charge generation and delocalization along and between the conjugated backbones occur. The polar side chains in OMIECs mostly enable ionic intercalation and sometimes side chains directly dope the polymer backbone. There is a lot of influence of side chain molecular design on the OMIEC properties specifically on ionic–electronic coupling and so forth.

(ii) **Block Copolymer:** In type-2; block copolymers remain phase segregated depending on the block lengths. In the P3HT-PSS block copolymer P3HT is electron conducting and PSS is ion conducting (Figure 2d). It is a largely disordered material, where small crystallites of  $\pi$ – $\pi$  stacked chains remain embedded into an amorphous matrix of PEDOT chains facilitating conduction of both electrons and ions (Figure 2e).<sup>9–18</sup> Recently we reported a novel water-soluble polythiophene graft block copolymer polythiophene-graft-poly (caprolactone-block-dimethyl aminoethyl methacrylate) (PTh-g-PCL-b-PDMAEMA, P1) using

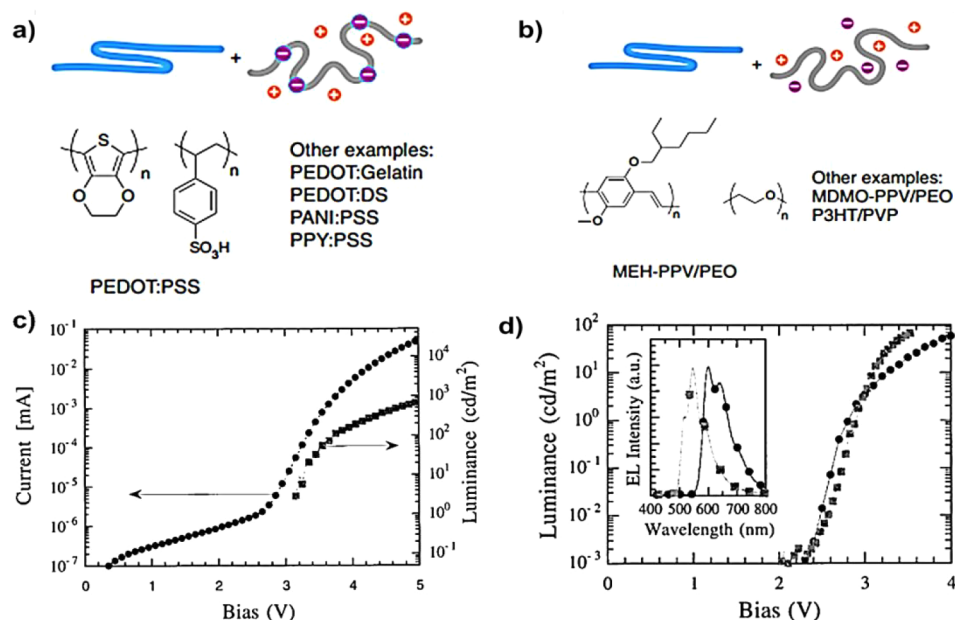


**Figure 3.** a) Heterogeneous blends of an electronically conducting conjugated polymer with an ionic charge bearing polyelectrolyte (PEDOT:PSS), b) heterogeneous blends of an electronically conducting conjugated polymer with an ion solvating solid polymer electrolyte (MEH-PPV/PEO), c) typical OMEIC type  $I$ - $V$  curve (○) of PPV:PEO:Li<sup>+</sup>, d) typical data for orange-red and green emitting LECs fabricated from MEH-PPV:PEO:Li<sup>+</sup> (○) and PPV:PEO:Li<sup>+</sup> (□) blend films. [Parts a and b reprinted with permission from ref 1a; parts c and d reprinted with permission from ref 7c.]

combined polymerization techniques (Figure 2f). The  $I$ - $V$  plot at pH-3 shows a clear signature of the OMEIC property as the  $-N(CH_3)_2$  group of P1 became protonated, resulting in the generation of ionic conductivity which shows a hike in current with an increase of voltage through proton hopping, and the electronic conductivity arises from the flow of electrons through the conjugated polythiophene chain.<sup>19</sup> At pH 7 the dimethyl amino group is not protonated so ionic flow is absent, showing no characteristics of OMEIC property. At pH 10, P1 shows an initial nonvariant  $I$ - $V$  plot, and then a small increase of current with increase of voltage is noted. Here, the current at +5 V ( $\sim 1.2 \times 10^{-7}$  A) is two times higher than the current (electronic) of pH 7 ( $0.6 \times 10^{-7}$  A). Most probably, this two-times higher current at pH 10 may arise from ionic contribution as during drying of ammonium hydroxide (used to make pH10), few  $NH_4^+$  ions may remain coordinated at  $-N(CH_3)_2$  centers and contribute to moderate ionic conductivity at +5 V. This type of OMEIC material finds extensive use in fluorescent biosensors and optoelectronic devices.

- (iii) **Copolymer with polymer electrolyte:** The grafted side chain moieties of the conducting polymer may also contain polymer electrolyte where external ion doping can impart ionic and electronic conductivity. An example of this type of OMEIC material is poly(2-(3,3'-bis(2-(2-(2-methoxyethoxy)-ethoxy) ethoxy)-[2,-bithiophene]-5-yl)thieno [3,2-*b*] thiophene) p(g2T-TT) (Figure 2c) where the glycolic side chain can solvate externally added ions. Poly (3-hexyl thiophene)-poly(ethylene oxide) (P3HT-PEO)

and its homologues are also good examples of conjugated polymer/polymer electrolyte block copolymers. The P3HT block is an electronically conducting block and PEO is an ionically conducting block when doped with alkali metal ions. Mesoscale morphological disorder produces extended, interconnected domains facilitating ionic and electronic transport. These types of OMEIC materials find uses in electrochromic, transistor, chemical sensor, and energy storage devices.<sup>1a</sup>

- (b) Blends of conjugated polymers:  
(i) Blends with polyelectrolyte or polymer electrolyte.

The most explored OMEIC in this category is the blend of conjugated polymer with polyelectrolyte. Here polystyrene sulfonate (PSS) is used to dope poly(3, 4-ethylenedioxythiophene) making PEDOT:PSS blend. PEDOT has poor solubility, so to ensure good dispersion it is polymerized into a template of polystyrene sulfonic acid, (PSS) (Figure 3a). It is a heterogeneous blend of a conducting polymer with an ionically conducting polyelectrolyte. The morphology of PEDOT:PSS OMEIC is governed by choices of solvents, cosolvents, blend ratios, and so forth. Aqueous PEDOT:PSS is generally mixed with a low amount of ethylene glycol to make well-connected ordered domains, improving the charge mobility but not upsetting the ionic transport. This is because the performance of OMEICs is closely related to the material microstructure. The OMEIC property of this PEDOT:PSS blend is mostly utilized in supercapacitors, electrochromic devices, neuro-morphic devices, biological sensors, and organic electrochemical transistors (OECTs).<sup>1a</sup>

Almost similar materials are blends of electronically conducting polymer and an ion solvating solid polymer electrolyte. The most common example is poly [2-methoxy-5-(2-ethylhexyloxy)-1,4-phenylenevinylene] (MEH-PPV)/poly



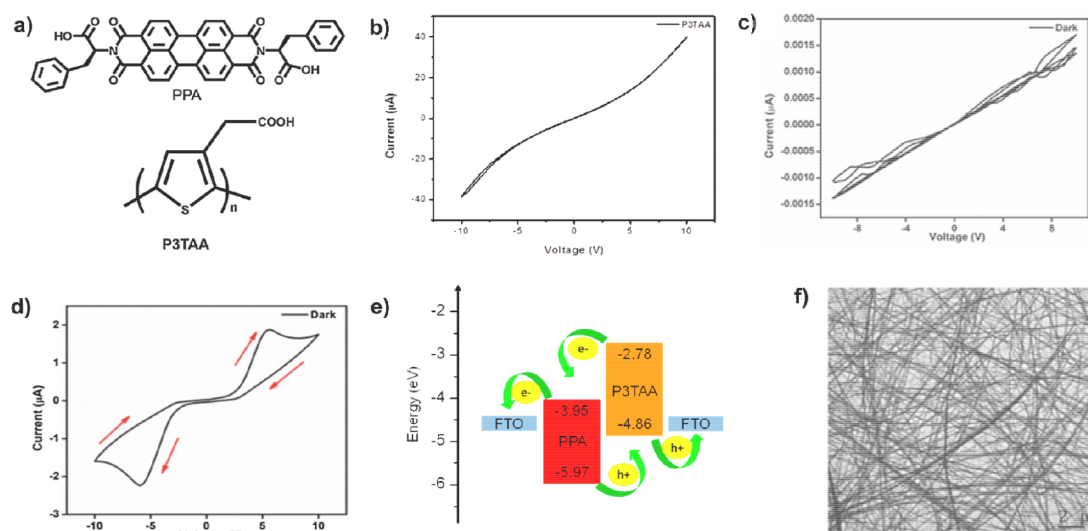


**Figure 4.** Donor–acceptor interaction in the PPA/P3TAA hybrid xerogel (from THF) showing OMEIC behavior. (a) Chemical structure of PPA and P3TAA, (b)  $I$ – $V$  curve of P3TAA, (c)  $I$ – $V$  curve of PPA, (d)  $I$ – $V$  curve of PPA/P3TAA hybrid (1:1) xerogel from THF, (e) energy diagram of PPA and P3TAA, and (f) TEM micrograph of PPA/P3TAA hybrid xerogel. Reprinted with permission from ref 2a.

(ethylene oxide) (PEO) (Figure 3b). This is produced by polymerization of MEH-PPV and subsequent mixing with PEO in a suitable solvent/cosolvent producing phase separated microstructures representing composites of light emitting electrochemical cell (LECs). Heeger and co-workers have found that a blend of PEO, containing lithium trifluoromethane sulfonate at the blend composition of PPV:PEO: Li<sup>+</sup> (5:5:1 by weight) exhibits a typical OMEIC type  $I$ – $V$  curve. The light illumination intensity, monitored with a calibrated Si photodiode, increases with an increase of voltage. This type of OMEIC material has found uses in light-emitting electrochemical cells (LECs). Heeger and co-workers have found that a blend of the semiconducting polymer, poly(phenylenevinylene) (PPV), with a polymer electrolyte showed a luminescence of 720 cd/m<sup>2</sup> at 5 V (Figure 3c).<sup>7c</sup> Electrochemical blends of PPV:PEO:Li<sup>+</sup> and MEH-PPV:PEO:Li<sup>+</sup> were used for green and orange-red light LECs (Figure 3c,d).

- (ii) Blends with small molecules, peptides, and so forth with a donor–acceptor molecular skeleton.

The OMEIC materials are classified as p-type or n-type, with p-type conducting polymers mostly represented by thiophene-based materials. Efficient n/p-type OMEICs are prepared using a donor–acceptor molecular skeleton bearing strong electron accepting rylene diimides, such as 1,4,5,8-tetracarboxylic acid diimide (NDI), perylene diimide. Blending of the NDI chromophore with polythiophene derivatives results in low oxidation/reduction potentials for the OMEIC copolymer. This enables the production of bipolar p- and n-type OMEIC materials.<sup>20</sup> In addition, copolymeric OMEICs containing an n-type NDI core, with a p-type building block (for example, polythiophene) are drawing much attention as electrons are effectively injected and delocalized along the copolymer chain, especially when ionically conductive side chains are utilized.<sup>21</sup>

Recently, a hybrid of *N,N*-di((*S*)-1-carboxylethyl)-3,4:9,10 perylene tetra carboxylic diimide (PTCDA, n-type semiconductor) with polyaniline (PANI, p-type semiconductor) made from dilute acetic acid medium at a 13 wt % concentration of PTCDA has been reported. The  $I$ – $V$

characteristic curve exhibits signature OMEIC properties under both dark and illuminated conditions. Here the PANI acts as an electronic conductor and the ionized protons of PTCDA act as an ionic conductor.<sup>2b</sup> Also a similar type p-n hybrid xerogel from THF and DMF was explored for the charge transport properties of PBI-acceptor and poly(3-thiophene acetic acid)(P3TAA-donor) composite. The *L*-phenyl alanine conjugated perylenebisimide (PPA) has a semiconductor property and forms gels in tetrahydrofuran (THF) and dimethyl formamide (DMF).<sup>2a</sup> The  $I$ – $V$  plot of P3TAA-PPA xerogel from THF exhibits a sharp increase of current at low voltage for both positive and negative bias under both dark and illuminated conditions, showing signature OMEIC properties. However, the xerogel from DMF exhibits only a typical semiconducting behavior. The presence of OMEIC property is also supported from the presence of Warburg impedance in its THF-xerogel systems but it is absent in DMF-xerogel systems. The working principle of donor-acceptor type OMEIC materials is illustrated using a PPA-P3TAA hybrid system cast from THF (Figure 4a). In both PPA and P3TAA there are carboxylic acid groups and the perylenebisimide of PPA is a good acceptor moiety, however the  $I$ – $V$  plots of pure components exhibit only a semiconducting nature (Figure 4b,c). But the P3TAA/PPA donor/acceptor hybrid xerogel made from THF exhibits a signature of OMEIC property for both positive and negative bias (Figure 4d). The HOMO and LUMO energy levels of PPA are  $-5.97$  eV and  $-3.95$  eV and for P3TAA they are  $-4.86$  eV and  $-2.78$  eV, respectively<sup>2a</sup> (Figure 4e). This band structure induces electron transfer from P3TAA to PPA and a hole transfer in the reverse direction, thus stimulating different electronic properties in the P3TAA/PPA hybrid than that of the components. Due to transfer of electrons from the donor P3TAA chain to the acceptor PPA moiety the carboxylic acid groups of the PTAAs in the hybrid become ionized and these protons exhibit ionic conductance. Thus the hybrid cast from THF exhibits an OMEIC nature with a sharp increase of current with voltage and a negative differential resistance (NDR) with further increase of voltage. The P3TAA-PPA xerogel from THF exhibits a highly dense fibrillar network

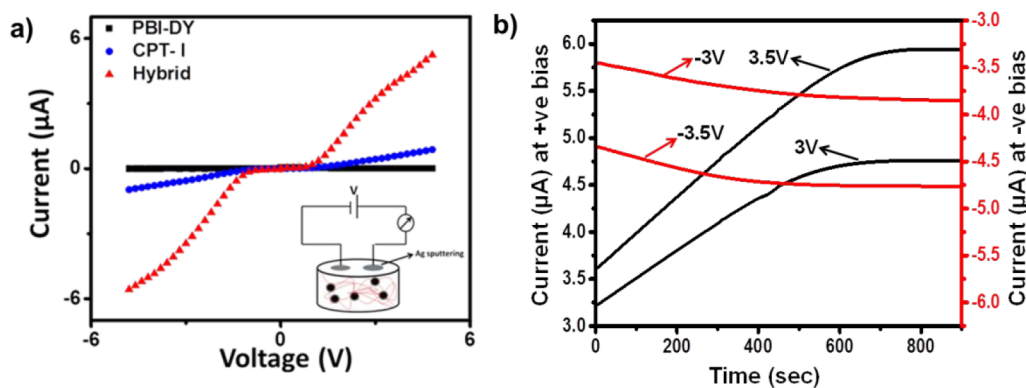


**Figure 5.** a) Current ( $I$ )-voltage ( $V$ ) behavior of CPT-I (blue dots), PBI-DY (black line), and the hybrid systems (red triangles). [Inset: Schematic set up of the  $I$ - $V$  measurement.]; b) current ( $I$ ) vs time ( $t$ ) plots of the CPT-I-PBI-DY hybrid at both positive (black line) and negative voltages (red line). [Parts a and b reprinted with permission from ref 8.]

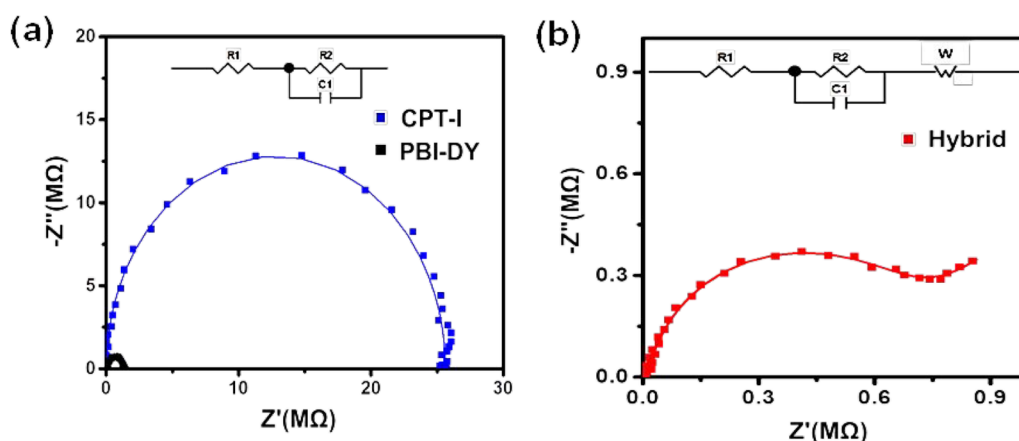


**Figure 6.** Nyquist plot from the impedance spectra of (a) CPT-I and PBI-DY and (b) the CPT-I-PBI-DY hybrid at 50 wt % PBI-DY. [Parts a and b reprinted with permission from ref 8.]

morphology (Figure 4f) causing easier hopping of ions carrying the charges showing OMEIC characteristics even at a lower voltage of both positive and negative bias. But the OMEIC property is absent in the P3TAA-PPA xerogel made from DMF because of the much lower density of the fibrillar network due to the high solvation power of DMF compared to that of THF.<sup>2a</sup>

In a recent report we made hybrids of a peptide conjugated with perylene bisimide (PBI-DY) (acceptor) with a polythiophene based cationic polymer (CPT-I, donor).<sup>8</sup> The  $I$ - $V$  measurements indicate the semiconducting nature of the samples; however, there is a difference in the hybrid from those of the components. With an increase of voltage, the hybrid shows a much sharper increase in current, behaving like an OMEIC material, where the contribution of both electronic and ionic conductivity plays an important role (Figure 5a). In order to find support the presence of ionic conductivity in the system current vs time ( $I$ - $t$ ) plots are made at a particular potential (Figure 5b) as for the high viscosity of the polymeric material the ionic conductance is not spontaneous like the electronic contribution during the  $I$ - $V$  measurement as voltage pulse is applied here for only 5 s.<sup>8</sup> Therefore at a particular bias, the current should vary with time depending on the charge nature, its size, and the applied voltage. Figure 5b shows that at +3.0 V the current increases linearly with time, showing a saturation value with an increase of current value of 1.5 mA

in 900 s, thereby leveling off. At -3 V the current shows a small decrease of 0.4 mA in 900 s at its saturation point. In 900 s at a higher bias of +3.5 V the current increases 2.25 mA at its leveling point and at the negative bias a similar linear decrease of current of 0.4 mA in 900 s is noted at the saturation point. The iodide ion of CPT-I in the hybrid is somewhat free due to the interaction between the quaternary ammonium ion and the carboxylate anion of PBI-DY. At positive bias, current increases with time for the flow of iodide ion while at negative bias a small decrease of current with time occurs due to retardation of the flow of iodide ion. The presence of ionic conductance in the CPT-I-PBI-DY hybrid is evident from the impedance data of the components and the hybrid (Figure 6a,b) and the Nyquist plots exhibit Warburg impedance in the hybrid for diffusion flow of ions, at a lower frequency region. However, the Warburg impedance is absent in the pure components suggesting that hybrid formation makes the iodide ion free to move under a particular bias causing the OMEIC property. The excellent photoswitching ON-OFF property under white light illumination of this system arises from the good donor-acceptor interaction between the components.<sup>8</sup>

(c) Nonconjugated polymer showing OMEIC property.

Radical polymers having the ability to produce ion and electron transporting materials have recently been made by blending a nonconjugated, amorphous, low-glass-transition temperature polymer poly(4-glycidyoxy-2,2,6,6-tetramethylpi-

peridine-1-oxyl) (PTEO) with an ionic dopant lithium bis(trifluoromethanesulfonyl)imide salt (LiTFSI).<sup>22</sup> PTEO has higher electrical conductivity ( $0.2 \text{ S cm}^{-1}$ ) because of the flexible macromolecular backbone and side-chain linker. Tuning the precise chemical nature of the radical pendant group using the ionic dopant is the key parameter for the increase of long-range electrical conductivity. Charge transport in PTEO is a result of a redox self-exchange reaction which is promoted by the movement of the pendant group and relaxation of the polymer main chain. The addition of the Li-salt to the PTEO matrix influences the chemical nature of the radical pendant group and the chain dynamics of the polymer, resulting in an increase of conductivity of the polymer across long channel lengths. Thus, complementary effects of radical polymer and ions result in electronic, ionic–electronic, and ionic conductivity. They have reported a maximum ionic conductivity of  $10^{-3} \text{ S cm}^{-1}$ . This finding demonstrates a different macromolecular design from the commonly accepted conjugated polymer compositions for making next-generation OMEIC materials.

## CONDUCTION MECHANISM IN OMIECS

The performance of OMIECs can be elucidated using organic electrochemical transistors (OECTs) because they provide a platform for both the electronic and ionic conductance. In OECTs, a gate voltage is applied causing the flow of ions through the mixed conductor resulting in a change in the oxidation state of the mixed conductor causing a difference in current. In OMIECs two different modes of operation, that is, accumulation and depletion take place. In the depletion mode, OMIECs exist in a doped state as in [PEDOT:PSS] at an unbiased state but on application of a bias, the doped ions are balanced by the migrating ions into the structure. This results in a reduction of the doping extent of the polymer backbone diminishing the measured current. But in the accumulation mode OMIECs remain in an undoped condition at an unbiased state. On application of a bias, ions travel into the OMIECs, thus doping the polymer and causing an increase of current.

Transconductance, a ratio of current response from the applied voltage, arising from the bulk doping for ion migration in OECTs is a commonly used parameter for organic field-effect transistors (OFETs). Transconductance is localized at the interface and is dependent on the thickness of the film. Hence, the equation for calculating transconductance is

$$g_m = \frac{Wd}{L} \mu C^* (V_{th} - V_g)$$

where  $g_m$  is the transconductance,  $d$  is the thickness of the film,  $W$  is the channel width,  $L$  is the length of the channel,  $\mu$  is the electronic mobility,  $V_{th}$  is the threshold voltage,  $C^*$  is the volumetric capacitance, and  $V_g$  is the gate voltage. It is evident from the equation that the device geometry influences the transconductance magnitude and hence the OMIEC property. Also an alternative way for evaluating OMIEC performance is the product  $\mu C^*$ , where  $\mu$  represents the electronic component, and  $C^*$  represents the ability of the polymer to interact with ions, signifying a steady-state performance of the device.<sup>9</sup> In Figure 7 the  $\mu$  vs  $C^*$  plot is shown, and it is evident that polymers even with lower electronic mobility can have a high  $\mu C^*$ , that is, transconductance with high volumetric capacitance. However, it does not indicate the speed of ionic

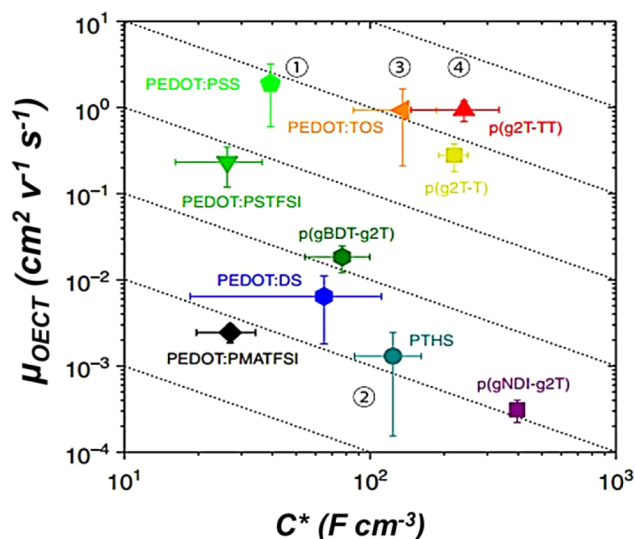


**Figure 7.**  $\mu_{\text{OECT}}-C^*$  map of 10 reported OMIEC materials. Dotted lines denote a constant  $\mu C^*$  product. [Reprinted with permission from ref. 9.]

uptake because these measurements are made for steady-state performance.

## PROCESSES IN OMIECS

**Ionic–Electronic Interactions.** The presence of an electronic charge in OMIECs requires stabilizing the excess ionic charge of the opposite sign and counterbalancing of the ionic charge with electronic charge is referred to as doping, resulting in an increase of electrical conductivity. The degree of doping can be modulated with an applied bias on coupling through an electrolyte. This results in a potential-dependent capacitance ( $C$ ) per volume or mass of the OMIEC, characterizing the strength of the ionic–electronic coupling. Homogeneous OMIECs exhibit larger ionic–electronic coupling and have higher values of volumetric capacitances than biphasic OMIECs.<sup>1a</sup> This potential-dependent coupling offers a fundamental mechanism of charge storage in OMIEC-based batteries, supercapacitors, and transducers. This coupling may also cause the filling or emptying of electronic states permitting the reversible removal of the color of optical transitions in electrochromical devices. Also modulation of the degree of doping changes the electrical conductivity producing different neuromorphic and OMIEC-based OECTs devices.

**Electronic Transport.** OMIECs mostly have an organic  $\pi$ -conjugated electronic structure containing a significant degree of structural disorder. The high degree of  $\pi$ -conjugation produces weakly bound electrons which move through the delocalized  $\pi$ -orbitals in the molecule, and intermolecular conduction occurs through  $\pi$ - $\pi$  overlap. Disorder disfavors the extent of delocalization and  $\pi$ - $\pi$  overlapping, promoting the charge transport through thermally activated hopping (Figure 8a) between distant favorable energy states. Both electronic charge carrier density and density of accessible hopping states are low without doping causing low electrical conductivity. Doping in OMIECs is present for the presence of ion–electron coupling. The dopant concentrations and charge carrier density may vary over many orders of magnitude. At very low concentrations the dopant ions act as Coulombic traps but with an increase of doping the activation energy of charge hopping decreases, and the carrier mobility also increases,



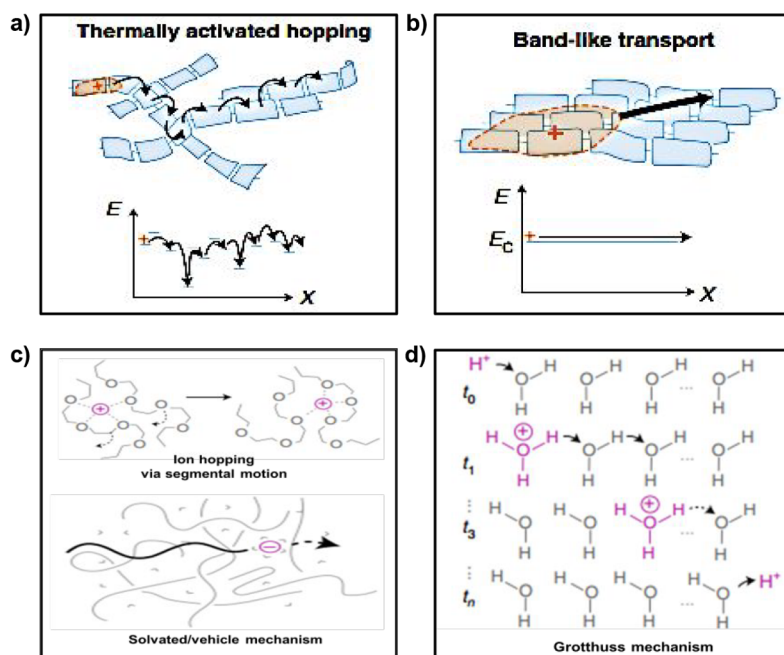


**Figure 8.** a) Thermally activated hopping transport of relatively localized electronic charge carriers between distant favorable energy states, b) diffused band-like transport of relatively delocalized electronic charge carriers, c) ionic charge transport through segmental motion-assisted ion hopping, and d) ionic charge transport through the Grotthuss mechanism of proton hopping. [Reprinted with permission from ref 1a.]

exhibiting diffuse band-like charge transport (Figure 8b). At very high doping levels, disorder increases causing carrier localization, which results in a plateau or reduction in the electronic charge carrier mobility. Nonconjugated radical polymers also play a role in thermally activated charge transfer between pendant radical sites along with local diffusion of polymer segments to bring radical sites closer for efficient charge transfer.<sup>22</sup>

**Ionic Transport.** The ability to conduct ionic currents makes OMIECs different from other  $\pi$ -conjugated organic semiconductors where only electronic current flow occurs. The ionic transport is complex in nature because ions can be multivalent, forming ion pairs and larger clusters; and they are sensitive to solvent and solvation. The ionic conductivity ( $\sigma_{\text{ionic}}$ ) is the sum of the ion conductance of each ionic species which is the sum of the products of the number density ( $n_i$ ), ion charge ( $z_i$ ), mobility ( $\mu_i$ ), and elementary charge ( $e$ ):

$$\sigma_{\text{ionic}} = \sum_i n_i |z_i| e \mu_i$$

Ion mobilities and diffusivities ( $D$ ) are interconvertible via Einstein relation:

$$D = \frac{\mu k_B T}{e}$$

where  $k_B$  is Boltzmann's constant and  $T$  is temperature.

In the case of dry OMIECs, ion transport is unipolar where one of the ionic charged species is fixed on a polyelectrolyte, and in other cases both anions and cations are mobile. OMIECs having contact with an electrolyte swell, allowing infiltration of excess ions and both anions and cations to contribute to ionic transport. In the dry state, ion movement occurs by ion hopping along with segmental motion of the side chains or backbone chain. Integration of ion-coordinating moieties may improve the segmental motion assisted transport

of ions (Figure 8c). OMIECs are highly sensitive to moisture, as contact with a liquid electrolyte swells them and ion transport occurs more rapidly via solvated ion vehicles. Electrolyte-swollen PEDOT:PSS exhibits solvated cation mobility. In water swollen OMIECs, proton conduction occurs rapidly via the Grotthuss mechanism (Figure 8d) of proton hopping between hydronium and water molecules. The relationship between ionic transport and ionic–electronic coupling is somewhat different from electronic charge transport. The external electrolyte contact of OMIECs can result in access to a large population of charge-balanced ions independent of ionic–electronic coupling.

**Directionality and Dimensionality.** The specific device geometry of OMIECs dictates the directionality and dimensionality of electron transport, ion transport, and electronic–ionic coupling.<sup>1a</sup> In thin film OMIECs, transport occurs in different length scales (nm to mm). Cyclic voltammetry and impedance experiments where OMIEC-coated electrodes are used involve parallel electronic and ionic transport within the thick films of thickness 10–100 nms. These thin film OMIEC layers are used in sensing, electrochromic, and energy storage devices, and here, ionic–electronic coupling uniformly occurs through the film at steady state. In light-emitting cells electronic and ionic transport also occurs in parallel, for different length scales when the cell is planar ( $\sim 10 \mu\text{m}$ ) or vertical ( $\sim 100 \text{nm}$ ). But here, ionic–electronic coupling is nonuniform in response to electric fields under operating conditions. Orthogonal mixed ionic–electronic conduction occurs in transistors where ion transport occurs vertically and electronic transport occurs laterally within the electrodes via the OMIEC film. Similarly, distribution of volumetric ionic–electronic coupling depends on the time scales and applied potentials governed by the operating conditions.

**Applications.** The OMIEC property of polymers is mostly applied in organic electrochemical transistors (OECTs),



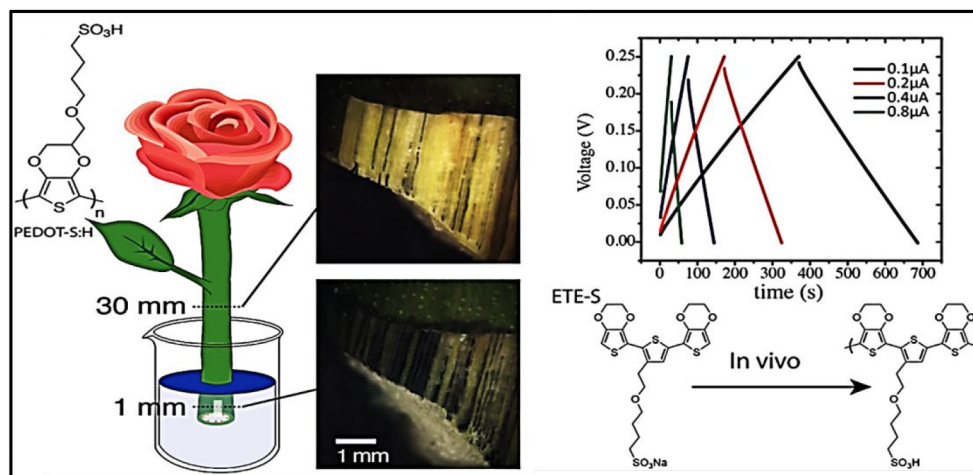


**Figure 9.** A common rose is used for fabrication of organic electronic devices, and typical charging–discharging curves for a rose supercapacitor. [Reprinted with permission from ref 18.]

electronic circuits, supercapacitors, batteries, photovoltaics, fuel cells, electro-chromic devices, light-emitting devices, bioelectronic devices, and so forth.<sup>14,20</sup> Here, a short account of each application is presented highlighting the importance of OMEIC materials.

**Circuits and Logic Gates.** The combination of high transconductance and ON/OFF ratios of OECTs with silicon-based integrated circuits promotes many applications, for example, internet connectivity and skin-patch applications. PEDOT:PSS OECT circuits are used in NAND and NOR logic gates.<sup>14,23</sup> Analog and logic OECT circuits find a variety of applications using different large-area and high-volume manufacturing techniques, such as screen printing, lamination, inkjet printing, and so forth. A voltage amplifier, combining a high-transconductance OECT with a resistor, enables improved recordings of electrocardiographic signals.

**Memory and Neuromorphic Devices.** There is a major interest in developing device networks involving the collocation of computation and memory. These systems are termed neuromorphic because they mimic the structure and function of the nervous system and they display temporary or permanent changes in electrical properties, thus simulating short or long-term memory. OECTs are interfaced with electrically active organs and tissues to monitor cell activity.<sup>14</sup> As an example, PEDOT:PSS OECTs microfabricated on parylene substrates can be located on the brain of a rat for recording of epileptic seizures. The signal-to-noise ratio is very good, hence activities from deep brain tissue can be recorded for local signal amplification. From the direct contact between the cerebro-spinal fluid and conducting channel, OECTs can be used to inject current locally to stimulate neurons. OECTs integrated with organic thin film transistors can be used as vanrecordmy organs in transgenic rats. They can record an electrocardiogram when placed on human skin and can further amplify recordings of electrophysiological signals from the human brain, heart, and muscle.<sup>14</sup>

**Bioelectronics.** OECTs have important roles in various bioelectronic devices for health care-related uses. In electrophysiology, OECTs are interfaced with electrically active tissues to measure cell activity.<sup>14</sup> In conjunction with cell cultures OECTs can also be used for drug screening, to monitor cell coverage, barrier tissue formation, and the cellular health of nonelectrogenic cells. OECT devices are used for the

detection of enteric pathogens in milk, by measuring transepithelial ion flow.<sup>14,20</sup> They are also applied to 3D cell culture models; OECTs when integrated with cyst-like 3D cultures are capable of monitoring their integrity and the effect of toxic compounds on the cell structure. OECTs fabricated with porous sponges of PEDOT:PSS can control 3D cell cultures.

In biosensors OECTs act as transducers for the detection of metabolites and electrolytes such as lactate and glucose, facilitating the monitoring of human health and performance.<sup>14</sup> For the detection of metabolites, selective interaction of a redox enzyme with a metabolite causes transfer of an electron to the gate of OECT. This changes the drain current depending on the metabolite concentration. Immobilization of the enzyme on the gate electrode leads to the formation of highly sensitive and selective sensors. The combination of OECTs with textiles finds uses in wearable applications, helping in the detection of analytes in sweat. There are many other applications of OECTs in saliva, breath, sweat, or cell culture,<sup>14,20</sup> and these applications make OECTs clinically relevant, like the use of OECT lactate sensors to measure the metastatic potential of tumor cells. OECTs are also used in the selective detection of dopamine and also for sensing of proteins, bacteria, and DNA and so forth.<sup>14,20</sup>

**Supercapacitor.** Supercapacitors possess high power density and excellent cycling stability, and thus play an important role in electrical vehicles. OMEIC devices are used in energy-storage technologies like supercapacitors. A composite system containing PEDOT:PSS, nanofibrillated cellulose (NFC), dimethyl sulfoxide (DMSO), and glycerol blended from solutions (NFC-PEDOT), exhibit high ionic and electronic conductivity and good mechanical properties well-matching with paper-making machines.<sup>15</sup> NFC improves the 3D micro/mesoscopic organization of PEDOT:PSS and glycerol improves the plasticity and hygroscopicity of the composite facilitating ions to move faster. The charging and discharging curves of a supercapacitor made from NFC-PEDOT electrodes store charge up to 1.2 C with a capacitance value, 2 F. A linear dependence of capacitance with NFC-PEDOT paper thickness indicates that the electrochemical reaction occurs at the bulk of electrodes. Chronoamperometric cycling runs indicate >99% retention of charge over 500 cycles. The composite shows good flexibility and water stability

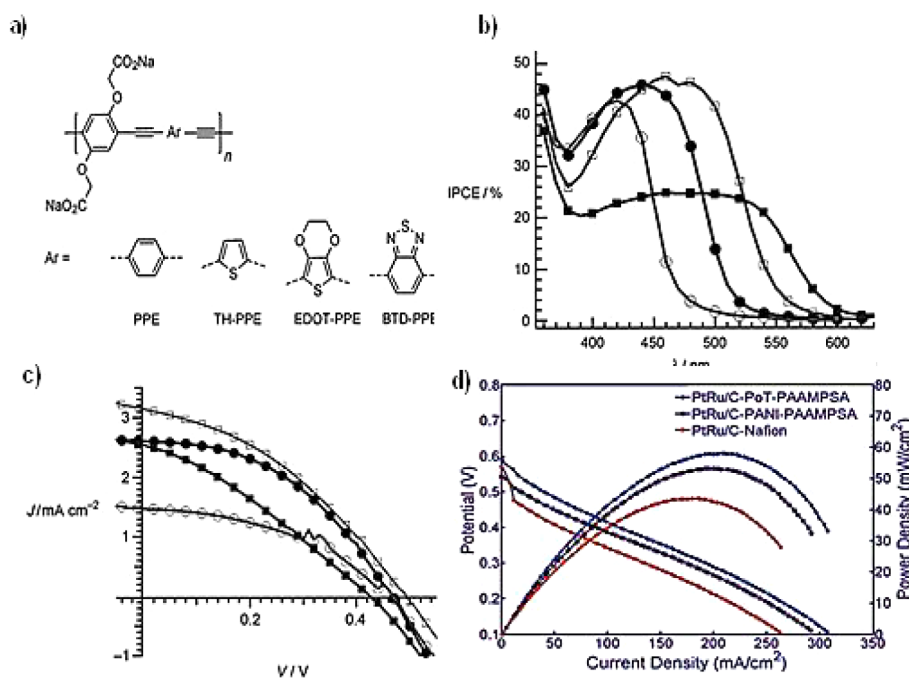


**Figure 10.** a) Structures of the repeat units for variable-gap PPE-based CPEs used in  $\text{TiO}_2$ -sensitized photovoltaic devices. b) Photocurrent action spectra of CPE-sensitized solar cells. c)  $J$ - $V$  characteristics of CPE-sensitized solar cells under AM1.5 conditions. (deg) PPE, (●) TH-PPE, (□) EDOT-PPE, (N) BTD-PP, d) single cell performances of DMFCs consisting of PtRu/C-PoT-PAAMPSA, PtRu/C-PANI-PAAMPSA, and PtRu/C-Nafion anode catalysts. [Parts a–c reprinted with permission from ref 23a; part d reprinted with permission from ref 23c.]

superior to that of pure PEDOT:PSS arising from the strong binding of the NFC fibrils on the PEDOT chains making it a useful supercapacitor. The potential-dependent ion-electron coupling is the basic mechanism of charge storage in OMIEC-based batteries and supercapacitors.

OMIECs can conduct electronic and ionic carriers in a tightly coupled fashion and its electronic interface with plants (**e-plants**) exhibits applications in energy storage. A common rose is used for fabrication of organic electronic (e-plant) devices where the plant's water transporting vascular tissue, xylem can absorb the OMIEC materials<sup>18</sup> (Figure 9). They have used ETE-S (an oligomer of PEDOT:PSS) which has preferable interaction between ETE-S, and the hydrophobic xylem surface allows the condensation of the molecule at the surface. The  $\pi$ - $\pi$  stacking of ETE-S oligomers facilitate formation of crystallites producing percolating paths for the charge carriers leading to the formation of long conducting wires with conductivities of  $10 \text{ S cm}^{-1}$  and a specific capacitance of  $20 \text{ F g}^{-1}$ . The xylem templated long conductors and the electrolyte rich environment is used for the fabrication of a supercapacitor along the stem as it exhibits very good stability and excellent charge retention, appraising the first demonstration of energy storage within a plant.

**Batteries.** In batteries inorganic ions ( $\text{M}^+$ ) move freely through the electrolyte from anode to cathode, and electrons flow in an external circuit from anode to cathode, producing power during discharge. During recharge, electrons and  $\text{M}^+$  flow in the reverse direction by an external voltage, storing electrical energy as chemical energy in the battery. Parameters, like gravimetric energy density ( $\text{mW h g}^{-1}$ ), volumetric capacity ( $\text{mA h cm}^{-3}$ ), gravimetric capacity ( $\text{mA h g}^{-1}$ ), rate capability, self-discharge characteristics, and cycling ability depend on the choice of battery design and battery materials.

OMIECs of conjugated polymers with polymer electrolytes and block copolymers have found uses in battery applications.

OMIECs are used as electrode binders in batteries, as they aid ion motion into and out of the electrode, and make electron extraction easy, improving the power density and stability. Because of their ductility the OMIECs help to alleviate the electrode fracture arising from the strain originating from the intercalation of the lithium ion. Incorporation of OMIECs increases the longevity and capacity of the battery significantly.<sup>3b</sup> For example, n-type terpolymer from alkyl-substituted fluorene copolymerized with fluorenone and methyl benzoate exhibits higher stability of the silicon electrode keeping a specific capacitance of  $2100 \text{ mA h g}^{-1}$  even after 650 cycles. Introducing the 3-D porous morphology of the binder/electrode mixture made of OMIEC with electrode show high-rate capabilities, for the conductive matrix and porosity facilitating greater electrolyte access to the electrode material.

**Solar Cell.** The research group of Reynolds and Schanze used the concept of spectral broadening using a dual-polymer system in a polymer-sensitized  $\text{TiO}_2$  solar cell by generating photocurrent from photoinduced electron transfer at the interface of the sensitizer polymers poly(phenylene-ethynylene, PPE) PPE- $\text{CO}_2$ , and polythiophene(PT) PT- $\text{CO}_2$ , and the acceptor,  $\text{TiO}_2$ , within the hybrid cells.<sup>23a24</sup> The LUMO levels are of higher energy from the conduction band of  $\text{TiO}_2$  in both polymers, so charge injection in  $\text{TiO}_2$  by the polymers is energetically favorable. As a result, the photocurrent ( $2.7 \text{ mA cm}^{-2}$ ) and power conversion efficiency ( $\eta = 0.9\%$ ) are obtained for the dual polymer solar cell. They used the same objective with a series of poly(arylene-ethynylene) conjugated polyelectrolytes substituted with carboxylic acid side groups (Figure 10a). A second arylene-ethynylene moiety of variable electron affinity is present in the PPE-based conducting

polymer electrolyte (CPE) yielding a variable HOMO–LUMO gap that varies, showing absorption maxima in the range 404 to 495 nm. The TiO<sub>2</sub> films when exposed to the CPEs solutions, polymers become adsorbed on the semiconductor surface, and more than 90% light absorption occurs corresponding to the band maximum of the polymers. A dye-sensitized solar cell (DSSC) fabricated with the TiO<sub>2</sub>/CPE films was fabricated using an I<sub>3</sub><sup>−</sup>/I<sup>−</sup> propylene carbonate electrolyte and Pt/FTO counter electrode. For each CPE, the incident photon to current conversion efficiency (IPCE) approaches 50% of absorption maximum for the CPEs (Figure 10 b). The photocurrent density and PCE at 1.5 AM illumination (Figure 10 c) increases in the order PPE < THPPE < EDOT-PPE, consistent with the red-shift in polymer absorption spectra. An interesting feature is that the IPCE and PCE for the TiO<sub>2</sub>/BTDPPE system are substantially lower than other CPEs. The decreased efficiency is due to exciton trapping in polymer aggregates; keeping the excitons in the film, and separated from the TiO<sub>2</sub> interface.

Films of PEDOT:PSS show high electronic conductivity and find uses for light-emitting diodes and solar cells.<sup>14</sup> A dye-sensitized solar cell (DSSC) fabricated with a conducting polymer (PANI, donor) and 5,5'-(1,3,5,7-tetraoxopyrrolo [3,4-*f*] isoindole-2,6-diyl) diisophthalic acid (P, acceptor) xerogel yield a power conversion efficiency (PCE) of 0.1%. But when PEDOT:PSS is used instead of PANI, the xerogel yields a higher PCE value of 0.27%. Using a strong acceptor like graphene oxide (GO) instead of P the DSSC of GO-PEDOT:PSS gel shows a much higher PCE of 3.25%. Further making a DSSC of trihybrid conducting xerogel consisting of P, GO, and PEDOT:PSS (GPPS) shows a maximum PCE of 4.5%. Here P and GO act as a joint acceptor but if we take the additive contribution of PCE of both individual acceptors with PEDOT:PSS then the total PCE of the trihybrid system should become 3.52%. So in the trihybrid gel (GPPS3) the PCE is higher by 1.0%, and it may be probable that PEDOT:PSS in the coassembled xerogel shows better OMEIC properties probably due to solvation of ions stimulating easier flow of charges causing increased PCE. The high PCE value and mechanically robust GPPS xerogel was used as a substitute for the active component TiO<sub>2</sub> of DSSC.<sup>23c</sup>

**Fuel Cell.** OMEIC materials are very efficiently used in fuel cells. Conducting polymer-like PANI have several beneficial contributions to direct methanol fuel cells (DMFC), but the applicability of PANI is limited by its insolubility in aqueous media. Doping of PANI with a proton conducting polymer acid, poly (2-acryl-amido- 2-methyl-1-propanesulfonic acid, (PAAMPSA) offers both high water dispersibility and high conductivity. Thus, PANI doped with PAAMPSA are suitable replacements for the expensive Nafion ionomers, in the anode of DMFC. Apart from PANI, poly(ortho-toluidine) (PoT)–PAAMPSA hybrid also exhibit very good performance (even better than PANI and Nafion composite).<sup>23d</sup> This is evident from the polarization curves (Figure 10d) of single cell DMFCs consisting of PtRu/C–PANI–PAAMPSA, PtRu/C–PoT–PAAMPSA, and PtRu/C–Nafion composite anodes, Pt/C–Nafion cathodes, and Nafion 115 membranes. PANI and PoT have higher electronic and ionic conductivity that comes from the PAAMPSA dopant ion as evident from impedance spectra. This polymeric ionomer shows higher performance in single cell DMFC compared to Nafion ionomers due to mixed ionic–electronic conduction, water dispersibility, and cocatalytic activity.<sup>23d</sup> In fuel cell energy generation, the air electrode,

which reduces oxygen, is a critical component in the device. Usually platinum (Pt) is used but Pt particles in the electrodes tend to be inactivated by carbon monoxide (CO). So, an air electrode made from a porous material coated with PEDOT (PEDOT/Goretex air electrode) acts as a good O<sub>2</sub> reduction catalyst. The O<sub>2</sub> conversion rates were comparable with those of Pt-catalyzed electrodes of similar geometry, and the electrode becomes insensitive to CO. This electrode shows continuous operation for 1500 h without material degradation. The catalytic property of PEDOT/Goretex air electrode can also be extended to other reactions like the hydrogen oxidation reaction in the fuel cell.

**Electrochromic Devices.** In electrochromic materials, a reversible color change takes place upon oxidation or reduction on passage of the electrical current at an appropriate electrode potential. PEDOT–PSS OMEIC is a good example of an electrochromic device when spin-coated on a commercial plastic transparency film.<sup>16</sup> Apart from the vascular tissue the leaves of rose through the stomata pores of leaf PEDOT:PSS are infiltrated with NFC, reaching the internal structure of the leaf. The self-organized 2D electrodes of PEDOT:PSS-NFC are free-standing and the pixels change color upon application of voltage exhibiting homogeneous electrochromism in the compartments on direct contact with the external electrodes. The type of electrochromism suggests mixed conduction within the compartments and pure ionic transport across the veins of the leaves.<sup>18</sup> The coloring and bleaching behavior of OMEICs for molecular tunability of conjugated polymers is applied to afford different colors. By fine-tuning of conjugated backbone of OMEIC, the entire color wheel (Figure 11) can

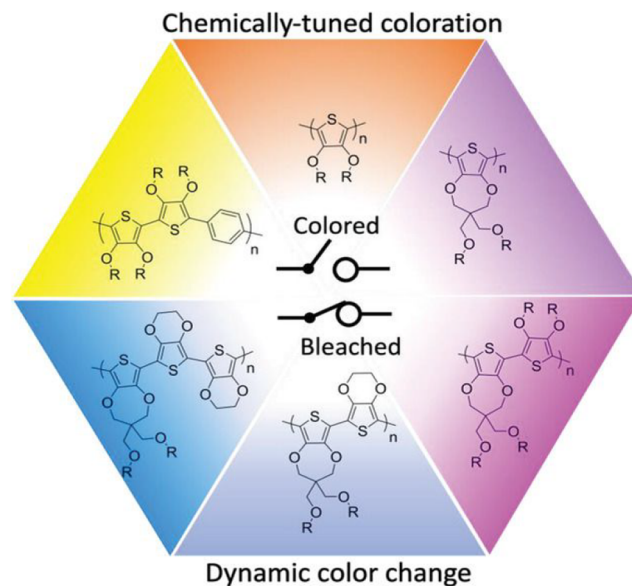


**Figure 11.** Illustration of color control in OMEICs through backbone and side chain engineering strategies. [Reprinted with permission from ref 21.]

be synthesized.<sup>21</sup> Such devices are useful in energy-saving-colored windows, full-color bistable displays, and dimmable goggles, glasses, and visors. A donor–acceptor approach is used to afford a myriad of colors, and backbone engineering strategies comprise tuning the core heterocycle choice as well as copolymerization. Apart from backbone engineering, the color of polymer OMEICs can be varied by a suitable choice of



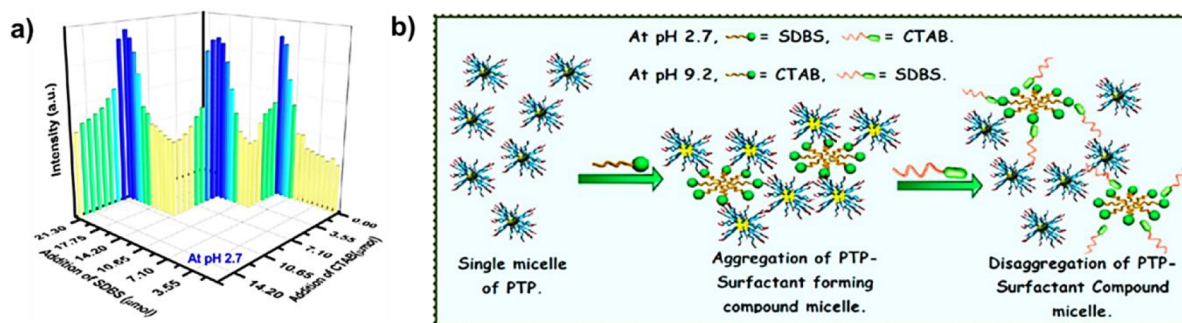


**Figure 12.** a) Reversible turn “on” and “off” plot of fluorescence intensity of PTP in aqueous solution with increasing amounts of SDBS then CTAB sequentially in pH 2.7 and b) schematic aggregation–disaggregation processes with enhancement and reduction of fluorescence of PTP with ionic surfactants at Acidic and Basic pH. Parts a and b reprinted with permission from ref 24a.]

side chains. The branched and bulky side chains of poly(alkoxythiophene) such as ethylhexyloxy are orange at neutral state but become red-shifted by replacing the branched side chains with hexagonally linked and more electron-rich ethylenedioxy to form PEDOT, forming a blue film. Changes in ionic and electronic charge density are the reason behind modulations in the electrochemical potential hence coloration.

**Light Emitting Devices.** The radiative recombination of electrons and holes emits light, and the phenomenon is known as electroluminescence where excited electrons release their energy as photons—light. In these devices, simultaneous *p*- and *n*-type doping on opposite sides of electrodes is in situ created where added ionic species provide the counterions necessary for doping. The orange red and green emitting light emitting cells (LECs) made with interdigitated electrodes are shown in Figure 3 with MEHPPV:PEO:Li<sup>+</sup> and PPV:PEO:Li<sup>+</sup> OMEIC materials. The luminance reaches 50–100 cd/m<sup>2</sup> at 3.5–4 V bias. The emission spectra (Figure 3 inset) of the emitted light are characteristic of emissions from MEH-PPV and PPV.<sup>7c</sup> Aqueous dispersions of PEDOT:PSS cast into films act as anodes for light-emitting diodes due to their high electronic (hole) conductivity.<sup>14</sup> During device operation, ion motion takes place with applied fields and anions and cations accumulate near the opposite electrode interfaces producing *p*–*i*–*n* junctions in conducting polymer–polymer electrolyte OMEIC films, however, the block-copolymer of a conducting polymer with polymer electrolyte produces *p*–*n* junctions.<sup>1a</sup> In light-emitting cells electronic and ionic transport occurs in parallel, over different length scales depending on vertical (~100 nm) or planar (~10 μm) conditions. The ion–electron coupling is nonuniform at steady-state in reaction to the applied electric field. A multilayer heterostructure of fluorene-based copolymer, PFO–PBD–NMe<sub>3</sub><sup>+</sup>, acts as an electron transport layer and PEDOT:PSS acts as a hole transport layer producing a polymer light emitting diode. It can operate at a low turn-on voltage (3 V) and at 6 V, the device displayed a brightness of 3450 cdm<sup>-2</sup> compared to 30 cdm<sup>-2</sup> for the device without the electron transport layer.<sup>23e</sup>

**Sensor Applications.** A variety of sensors can be formulated using OMEICs in different transduction modes like conductometric, amperometric, potentiometric, and colorimetric modes. The conductometric mode exploits electrical conductivity; amperometric sensing utilizes the current generated by redox reaction of an analyte at the working electrode, potentiometric sensing exploits changes in chemical potential by the analyte at open circuit; and colorimetric/fluorometric sensors use optical absorption/

fluorescence characteristics, which is governed by the local electronic structure. OMEICs like PEDOT:PSS and its derivatives are mostly used as sensors and when soaked into cotton fibers form an OECT channel that can be used for saline sensing.<sup>14</sup> In combination with nano fibrillated cellulose (NFC), PEDOT:PSS produces large-scale OECT systems, showing transconductance beyond 1 S when infused into living plants, which can be used to monitor plant growth. The ability to solvate ions makes OMEICs an ideal material to detect the concentration of ions in aqueous analytes according to the Nernst equation and this potential is measured with a reference electrode. This facilitates OMEICs as an electrode material for ionic sensors to detect Na<sup>+</sup>, K<sup>+</sup>, Ca<sup>2+</sup>, Mg<sup>2+</sup>, NH<sub>4</sub><sup>3+</sup>, and so forth.<sup>21</sup> OMEICs functionalized with ligands can bind neutral molecules and binding of these analytes increases the impedance, pH, or optical properties, making it an easy tool to detect a variety of chemical inputs extending its application in long-term environmental and health monitoring devices. OMEIC fluorescent sensors operate either in “turn-on” or “turn-off” modes.<sup>23e</sup> The turn-on and turn-off responses occur by various processes like redistribution of quencher ions between the analyte and polymer, variation of aggregation structure and/or conformation of the OMEIC polymer. Nandi and co-workers<sup>24a</sup> recently reported a series of work in this regard and a good example is polythiophene-graft-polyampholyte (PTP) which exhibits aqueous solubility with formation of small sized micellar aggregates with polythiophene at the center and radiating polyionic side chains (anionic or cationic for different pH of the medium) at the outer periphery. PTP shows reversible on and off fluorescence in both acidic and basic media on chronological addition of differently charged ionic surfactants, repeatedly. The fluorescence intensity of PTP at pH 2.7 increases with the addition of an anionic surfactant, sodium dodecyl benzene sulfonate (SDBS), due to the self-aggregation forming compound micelles (Figure 12). The fluorescence intensity again decreases on addition of a cationic surfactant, cetyltrimethylammonium bromide (CTAB), for aggregation of SDBS with CTAB, thus disassembling the PTP–SDBS aggregates. At pH 9.2, PTP also exhibits these turn on and turn off modes with the sequential insertion of cationic surfactant (CTAB) and anionic surfactant (SDBS), respectively. Similar fluorometric/colorimetric detection of RNA and the toxic cyanide ions using ionic polythiophenes is reported by the same group.<sup>24b,c</sup> There is clearly a wide variety of major applications for polymeric OMEIC materials.

**Outlook.** OMEIC materials are now mostly applied in the energy sector, electronic materials, biotechnology, sensors, and



so forth. Therefore, establishing structure–property relations of OMEICS is an exciting research field. Main chain engineering by making blocks of different conducting moieties (electronic or ionic) and side chain engineering in conducting polymers are very much needed to improve OMEIC properties. This is an interesting field particularly for synthetic polymer chemists as judicious choice of different monomers and side chain groups along with their composition is important. Apart from making blends of conducting polymers with polymer electrolytes or with molecules, having donor–acceptor architecture is very important to produce new OMEIC materials. Since electronic conductivity depends on the delocalization of charges along the main chain and ionic conductivity depends on solvation, the processing of these polymers in different shape, morphology, structure, and so forth are very much essential, so there is a great scope for polymer physical chemists to make blends and to control the polymer micro and meso structures on which both ionic and electronic conductivity and ion–electron coupling depend. Polymer physicists would require a great deal of work to understand the conduction mechanism of ions and electrons and to understand ion–electronic coupling as it dictates the specific use of the OMEIC for a desired purpose. Finally, it is the collective effort of material scientists, biologists, and technologists to make devices for the different applications discussed above and also to find new applications. So, more rigorous fundamental, synthetic, and structural works are necessary across the burgeoning field of OMEIC materials aimed at new and targeted applications.

## AUTHOR INFORMATION

### Corresponding Authors

**Arun K. Nandi** – Polymer Science Unit, School of Materials Science, Indian Association for the Cultivation of Science, Kolkata 700 032, India; [orcid.org/0000-0002-2099-452X](https://orcid.org/0000-0002-2099-452X); Email: [psuakn@iacs.res.in](mailto:psuakn@iacs.res.in)

**Arindam Banerjee** – School of Biological Science, Indian Association for the Cultivation of Science, Kolkata 700 032, India; [orcid.org/0000-0002-1309-921X](https://orcid.org/0000-0002-1309-921X); Email: [bcab@iacs.res.in](mailto:bcab@iacs.res.in)

### Author

**Soumyajit Hazra** – Polymer Science Unit, School of Materials Science, Indian Association for the Cultivation of Science, Kolkata 700 032, India; School of Biological Science, Indian Association for the Cultivation of Science, Kolkata 700 032, India; [orcid.org/0000-0001-7744-0117](https://orcid.org/0000-0001-7744-0117)

Complete contact information is available at: <https://pubs.acs.org/10.1021/acsomega.2c04516>

### Notes

The authors declare no competing financial interest.

### Bioographies

Mr Soumyajit Hazra received his M. Sc degree in Chemistry from Indian Institute of Engineering Science and Technology, Shibpur, India in 2016, and since then he is pursuing Ph.D under the joint supervision of Prof. Arindam Banerjee and Prof. Arun K. Nandi, at the Indian Association for the Cultivation of Science as a UGC fellow. His current research interests focus on optoelectronic properties of polymer-peptide conjugates.

Prof. Arindam Banerjee received Ph.D from Indian Institute of Science, Bangalore, India in 1997. He joined as a lecturer in Indian

Association for the Cultivation of Science, Calcutta in June, 1998 after brief post-doctoral research from Weizmann Institute of Science, Israel. He became a full professor in December of 2009. He has published 153 research papers in various peer reviewed international journals and has supervised 21 Ph.D. candidates. His current research interest includes peptide based soft functional materials, nanohybrids, nanoclusters, and carbon nanodots. He is an Editorial Advisory Board member in Soft Matter, A RSC journal. He is a fellow of the Indian Academy of Sciences (Bangalore) and also a Fellow, Royal Society of Chemistry (RSC), U.K. (2014).

Prof. Arun K. Nandi obtained his PhD degree on “Thermodynamics of Polymer–Polymer and Polymer–Solvent Mixing” by working at Indian Association for the Cultivation of Science (IACS) and joined the Chemistry Department, North Bengal University, Darjeeling. He did postdoctoral work at the Florida State University with Prof. L. Mandelkern in the crystallization of polymers. In 1992, he joined the Polymer Science Unit of IACS and he retired from the senior Professor position in February, 2019. Presently, he is Emeritus Scientist (CSIR) at IACS. His research interests focus on polymer blends, polymer crystallization, polymer and supramolecular gels, polymer nanocomposites, polymer synthesis, biomolecular hybrids, supercapacitors and polymer photovoltaics. He is the author of 247 papers, 5 book chapters, and a text book “Polymer Functionalized Graphene” (RSC, 2021) and has supervised 36 PhD students to date.

## ACKNOWLEDGMENTS

We gratefully acknowledge CSIR, New Delhi (ES grant (21(1055)/18-EMR-II)) for financial support.

## REFERENCES

- (1) (a) Paulsen, B. D.; Tybrandt, K.; Stavrinidou, E.; Rivnay, J. Organic Mixed Ionic–Electronic Conductors. *Nat. Mater.* **2020**, *19*, 13–26. (b) Huang, F.; Wu, H.; Cao, Y. Water/Alcohol Soluble Conjugated Polymers as Highly Efficient Electron Transporting/Injection Layer in Optoelectronic Devices. *Chem. Soc. Rev.* **2010**, *39*, 2500–2521.
- (2) (a) Chal, P.; Shit, A.; Levy, D.; Das, S.; Mondal, S.; Nandi, A. K. Effect of Molecular Packing on Modulation of Electronic Properties of Organic Donor–Acceptor Hybrid Gels. *Colloids Surfaces A* **2019**, *577*, 480–492. (b) Chal, P.; Shit, A.; Nandi, A. K. Dye-Sensitized Solar Cell from a New Organic n-Type Semiconductor/Polyaniline Composite: Insight from Impedance Spectroscopy. *J. Mater. Chem. C* **2016**, *4*, 272–285.
- (3) (a) Zeglio, E.; Schmidt, M. M.; Thelakkat, M.; Gabrielsson, R.; Solin, N.; Inganäs, O. Conjugated Polyelectrolyte Blends for Highly Stable Accumulation-Mode Electrochemical Transistors. *Chem. Mater.* **2017**, *29*, 4293–4300. (b) Onorato, J. W.; Luscombe, C. K. Morphological Effects on Polymeric Mixed Ionic/Electronic Conductors. *Mol. Syst. Des. Eng.* **2019**, *4*, 310–324.
- (4) (a) Patel, S. N.; Javier, A. E.; Stone, G. M.; Mullin, S. A.; Balsara, N. P. Simultaneous Conduction of Electronic Charge and Lithium Ions in Block Copolymers. *ACS Nano* **2012**, *6*, 1589–1600. (b) Moon, H. C.; Kim, J. K. Phase Segregation of Poly (3-Dodecylthiophene)-Block-Poly (Methyl Methacrylate) Copolymers. *Polymer* **2013**, *54*, 5437–5442. (c) Gu, Z.; Kanto, T.; Tsuchiya, K.; Ogino, K. Synthesis of Poly (3-hexylthiophene)-*b*-poly (ethylene oxide) for application to photovoltaic device. *J. Photopolym. Sci. Technol.* **2010**, *23*, 405–406.
- (5) Mukherjee, P.; Dawn, A.; Nandi, A. K. Biomolecular Hybrid of Poly (3-Thiophene Acetic Acid) and Double Stranded DNA: Optical and Conductivity Properties. *Langmuir* **2010**, *26*, 11025–11034.
- (6) Chung, J.; Khot, A.; Savoie, B. M.; Boudouris, B. W. 100th Anniversary of Macromolecular Science Viewpoint: Recent Advances and Opportunities for Mixed Ion and Charge Conducting Polymers. *ACS Macro Lett.* **2020**, *9*, 646–655.

- (7) (a) Riess, I. Polymeric Mixed Ionic Electronic Conductors. *Solid State Ionics* **2000**, 136–137, 1119–1130. (b) Riess, I.; Cahen, D. Analysis of Light Emitting Polymer Electrochemical Cells. *J. Appl. Phys.* **1997**, 82, 3147–3151. (c) Yu, G.; Pei, Q.; Heeger, A. J. Planar Light-Emitting Devices Fabricated with Luminescent Electrochemical Polyblends. *Appl. Phys. Lett.* **1997**, 70, 934–936. (d) Pei, Q.; Yu, G.; Zhang, C.; Yang, Y.; Heeger, A. J. Polymer Light-Emitting. *Science* **1995**, 269, 1086–1088.
- (8) Hazra, S.; Shit, A.; Ghosh, R.; Basu, K.; Banerjee, A.; Nandi, A. K. Modulation of the Optoelectronic Properties of a Donor-Acceptor Conjugate between a Cationic Polythiophene and a Peptide Appended Perylene Bisimide Amphiphile. *J. Mater. Chem. C* **2020**, 8, 3748–3757.
- (9) Inal, S.; Malliaras, G. G.; Rivnay, J. Benchmarking Organic Mixed Conductors for Transistors. *Nat. Commun.* **2017**, 8, 1767.
- (10) Khodagholy, D.; Doublet, T.; Quilichini, P.; Gurfinkel, M.; Leleux, P.; Ghestem, A.; Ismailova, E.; Hervé, T.; Sanaur, S.; Bernard, C.; Malliaras, G. G. In Vivo Recordings of Brain Activity Using Organic Transistors. *Nat. Commun.* **2013**, 4, 1575.
- (11) Lin, P.; Yan, F.; Yu, J.; Chan, H. L. W.; Yang, M. The Application of Organic Electrochemical Transistors in Cell-Based Biosensors. *Adv. Mater.* **2010**, 22, 3655–3660.
- (12) Williamson, A.; Rivnay, J.; Kergoat, L.; Jonsson, A.; Inal, S.; Uguz, I.; Ferro, M.; Ivanov, A.; Sjöström, T. A.; Simon, D. T.; Berggren, M.; Malliaras, G. G.; Bernard, C. Controlling Epileptiform Activity with Organic Electronic Ion Pumps. *Adv. Mater.* **2015**, 27, 3138–3144.
- (13) Kim, S. H.; Hong, K.; Xie, W.; Lee, K. H.; Zhang, S.; Lodge, T. P.; Frisbie, C. D. Electrolyte-Gated Transistors for Organic and Printed Electronics. *Adv. Mater.* **2013**, 25, 1822–1846.
- (14) Rivnay, J.; Inal, S.; Salleo, A.; Owens, R. M.; Berggren, M.; Malliaras, G. G. Organic Electrochemical Transistors. *Nat. Rev. Mater.* **2018**, 3, 17086.
- (15) Malti, A.; Edberg, J.; Granberg, H.; Khan, Z. U.; Andreasen, J. W.; Liu, X.; Zhao, D.; Zhang, H.; Yao, Y.; Brill, J. W.; Engquist, I.; Fahlman, M.; Wågberg, L.; Crispin, X.; Berggren, M. An Organic Mixed Ion-Electron Conductor for Power Electronics. *Adv. Sci.* **2016**, 3, 1500305.
- (16) Mortimer, R. J.; Dyer, A. L.; Reynolds, J. R. Electrochromic Organic and Polymeric Materials for Display Applications. *Displays* **2006**, 27, 2–18.
- (17) Haines, C. S.; Lima, M. D.; Li, N.; Spinks, G. M.; Foroughi, J.; Madden, J. D. W.; Kim, S. H.; et al. Artificial Muscles from Fishing Line and Sewing Thread. *Science* **2014**, 343, 868–872.
- (18) Berggren, M.; Crispin, X.; Fabiano, S.; Jonsson, M. P.; Simon, D. T.; Stavrinidou, E.; Tybrandt, K.; Zozoulenko, I. Ion Electron-Coupled Functionality in Materials and Devices Based on Conjugated Polymers. *Adv. Mater.* **2019**, 31, 1805813.
- (19) Haldar, U.; Mondal, S.; Hazra, S.; Guin, S.; Yeasmin, L.; Chatterjee, D. P.; Nandi, A. K. Tailor Made Synthesis of Water-Soluble Polythiophene-Graft-Poly(Caprolactone-Block-Dimethylaminoethyl Methacrylate) Copolymer and Their PH Tunable Self-Assembly and Optoelectronic Properties. *Eur. Polym. J.* **2022**, 168, 111124.
- (20) He, Y.; Kukhta, N. A.; Marks, A.; Luscombe, C. K. The Effect of Side Chain Engineering on Conjugated Polymers in Organic Electrochemical Transistors for Bioelectronic Applications. *J. Mater. Chem. C* **2022**, 10, 2314–2332.
- (21) Tan, S. T. M.; Gumyusenge, A.; Quill, T. J.; LeCroy, G. S.; Bonacchini, G. E.; Denti, I.; Salleo, A. Mixed Ionic–Electronic Conduction, a Multifunctional Property in Organic Conductors. *Adv. Mater.* **2022**, 34, 2110406.
- (22) Yu, I.; Jeon, D.; Boudouris, B.; Joo, Y. Mixed Ionic and Electronic Conduction in Radical Polymers. *Macromolecules* **2020**, 53, 4435–4441.
- (23) (a) Jiang, H.; Taranekekar, P.; Reynolds, J. R.; Schanze, K. S. Conjugated Polyelectrolytes: Synthesis, Photophysics, and Applications. *Angew. Chem., Int. Ed.* **2009**, 48, 4300–4316. (b) Das, S.; Chakraborty, P.; Shit, A.; Mondal, S.; Nandi, A. K. Robust hybrid hydrogels with good rectification properties and their application as active materials for dye-sensitized solar cells: insights from AC impedance spectroscopy. *J. Mater. Chem. A* **2016**, 4, 4194–4210. (c) Murthy, A.; Manthiram, A. Highly water-dispersible, mixed ionic–electronic conducting, polymer acid-doped polyanilines as ionomers for direct methanol fuel cells. *Chem. Commun.* **2011**, 47, 6882–6884. (d) Winther-Jensen, B.; Winther-Jensen, O.; Forsyth, M.; MacFarlane, D. R. High Rates of Oxygen Reduction over a Vapor Phase–Polymerized PEDOT Electrode. *Science* **2008**, 321, 671–674. (e) Jiang, H.; Zhao, X.; Shelton, A. H.; Lee, S. H.; Reynolds, J. R.; Schanze, K. S. Variable-Band-Gap Poly(arylene ethynylene) Conjugated Polyelectrolytes Adsorbed on Nanocrystalline TiO<sub>2</sub>: Photocurrent Efficiency as a Function of the Band Gap. *ACS Appl. Mater. Interfaces* **2009**, 1, 381–387.
- (24) (a) Ghosh, R.; Das, S.; Chatterjee, D. P.; Nandi, A. K. Surfactant-Triggered Fluorescence Turn “on/off” Behaviour of a Polythiophene-Graft-Polyampholyte. *Langmuir* **2016**, 32, 8413–8423. (b) Ghosh, R.; Chatterjee, D. P.; Das, S.; Mukhopadhyay, T. K.; Datta, A.; Nandi, A. K. Influence of Hofmeister I—On Tuning Optoelectronic Properties of Ampholytic Polythiophene by Varying pH and Conjugating with RNA. *Langmuir* **2017**, 33, 12739–12749. (c) Ghosh, R.; Das, S.; Chatterjee, D. P.; Nandi, A. K. Cationic polythiophene for specific detection of cyanide ions in water using fluorometric technique. *RSC Adv.* **2015**, 5, 92564–92572.